Electronic Supplementary Material (ESI) for Physical Chemistry Chemical Physics.

Supporting Information

Mechanistic insight into the destabilization of p53TD tetramer by cancer-related R337H mutation: a molecular dynamic study

Yawei Yu, Xuewei Dong, Yiming Tang, Le Li and Guanghong Wei*

Department of physics, State Key Laboratory of Surface Physics, and Key Laboratory for Computational Physical Sciences (Ministry of Education), Fudan University, Shanghai 200438, People's Republic of China.

E-mail: ghwei@fudan.edu.cn

This supporting material contains 15 supplemental figures (Figs. S1-S15).

Unless specified, all the results presented below are obtained using the data from five independent MD runs.

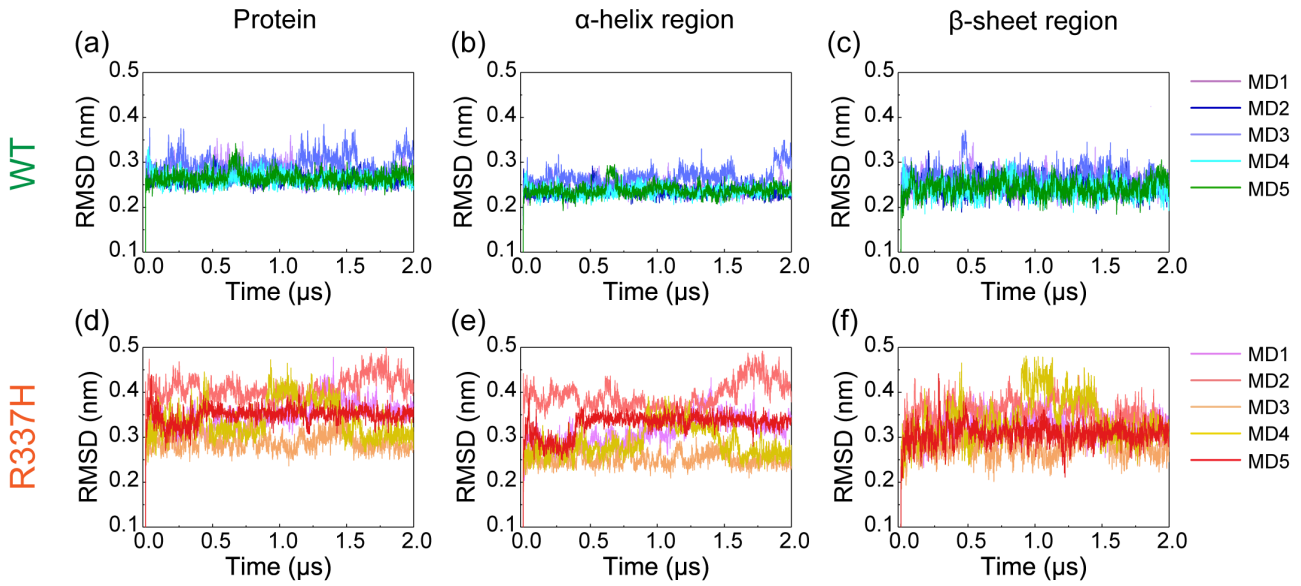

Fig. S1 Time evolution of the all-atom RMSD values of total protein, α-helix region and β-sheet region relative to their initial conformations of WT-p53Tet (a−c) and R337H-p53Tet (d−f).

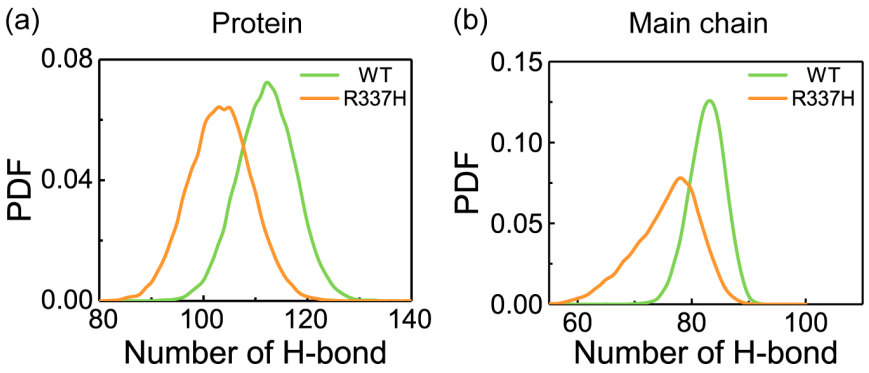

Fig. S2 The probability density function (PDF) of the Hydrogen bond (H-bond) number of total protein (a) and main chain (MC) (b) for WT-p53Tet and R337H-p53Tet.

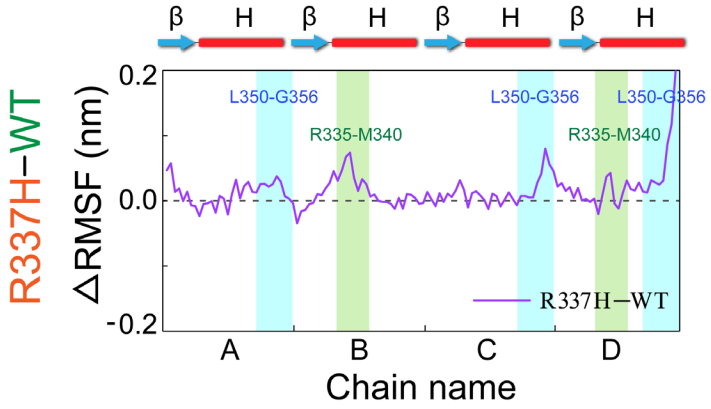

Fig.S3 The difference of residue-based RMSF values between R337H-p53Tet and WT-p53Tet (i.e. R337H-p53Tet minus WT-p53Tet). Two regions (L350-G356 and R335-M340) in R337H mutant have relatively large RMSF values.

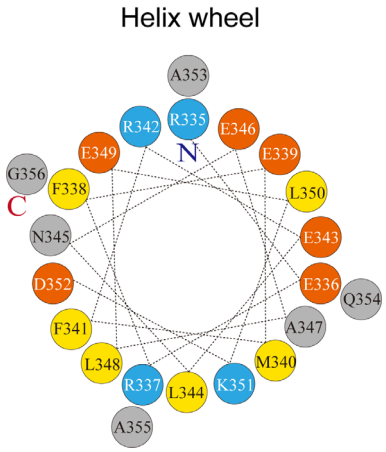

Fig. S4 The schematic diagram of α-helix wheel. The dash line manifests the sequence of amino sequence. Light blue: positively charged amino acids, orange: negatively charged amino acids, yellow: nonpolar amino acids, gray: polar amino acids.

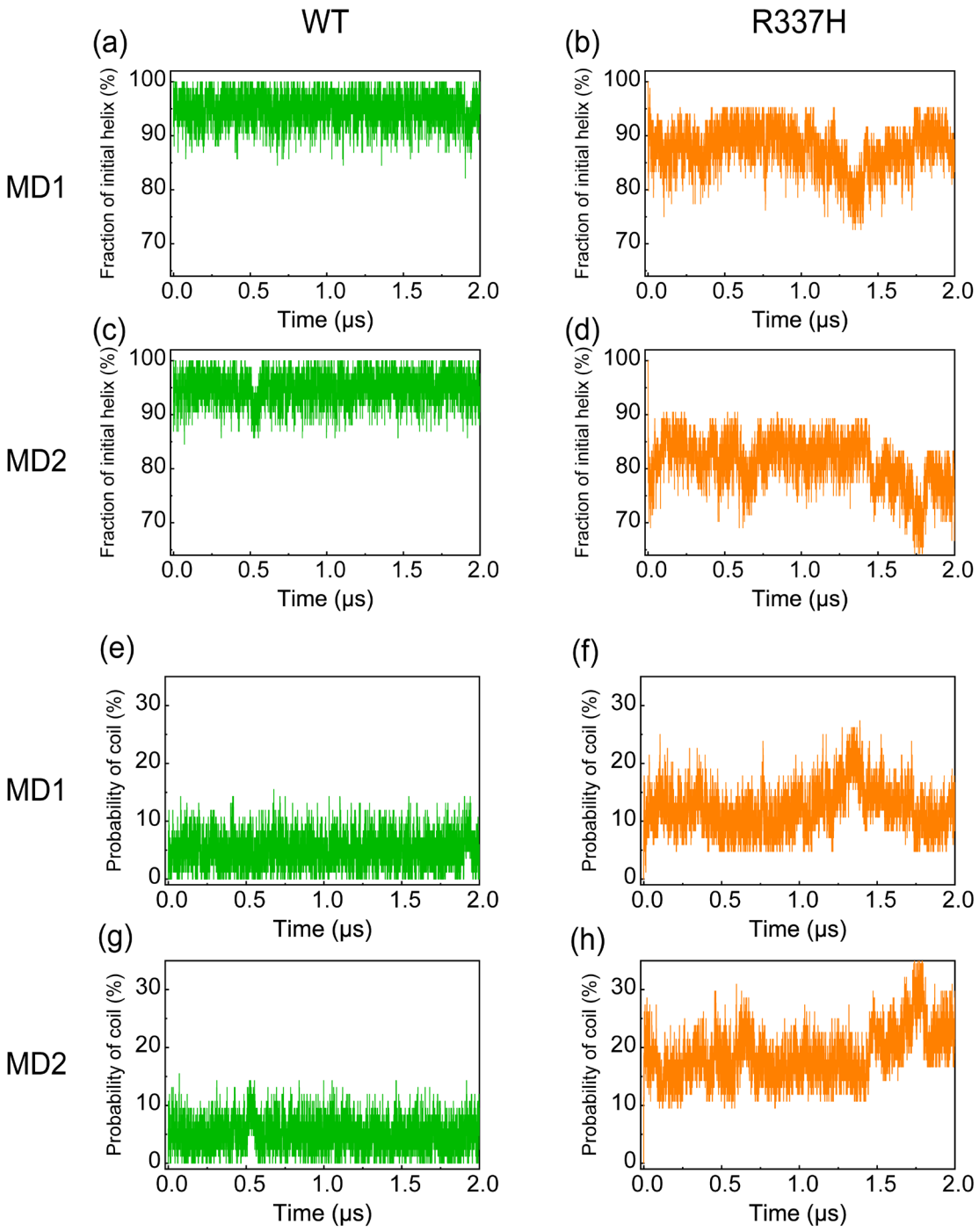

Fig. S5 The probability of dominant secondary structure in α-helix region as a function of time in two representative simulations. (a-d) The fraction of initial α-helix. (e-h) The probability of disordered coil conformation in α-helix region.

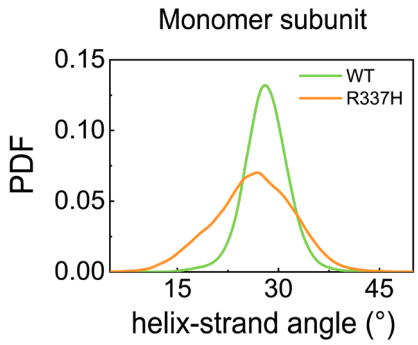

Fig. S6 The PDF of the angle between β-strand and α-helix in monomer subunit.

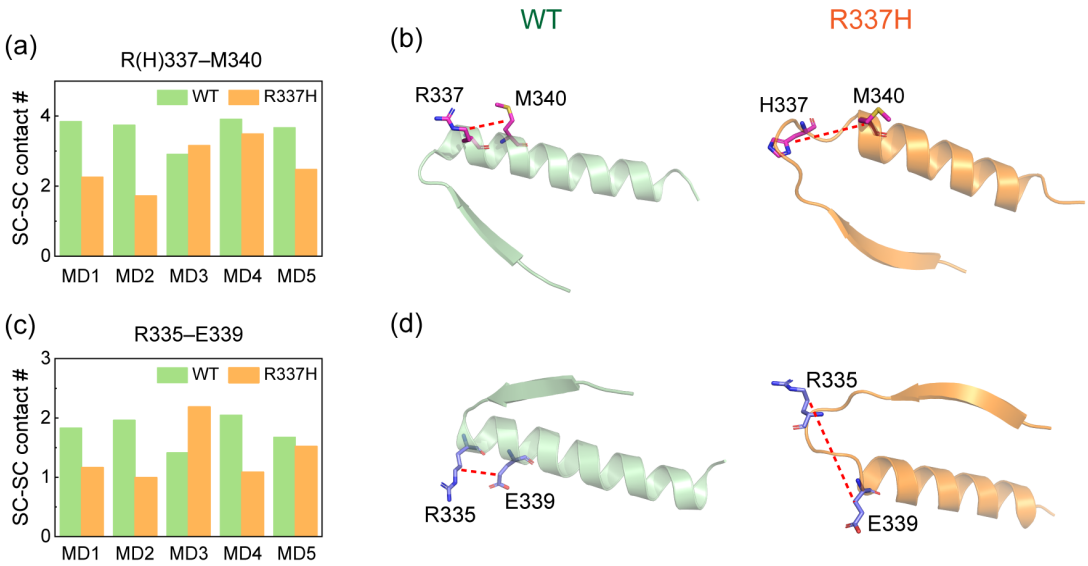

Fig. S7 Contact number of the side chain (SC) aliphatic hydrocarbons between residue R(H)337 and M340 (a) and between residue R335 and E339 (c). The snapshots show the distance change of aliphatic hydrocarbons of R(H)337-M340 residue pair (b) and R335-E339 residue pair (d).

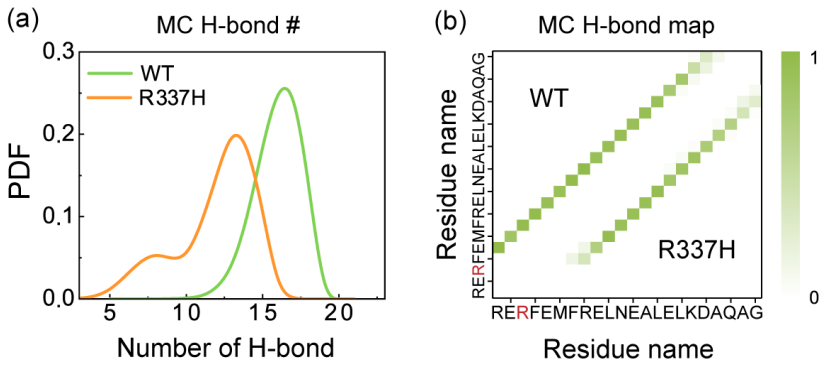

Fig. S8 The PDF of MC H-bond number of intra-helix in monomer subunit (a). The MC H-bond number map of intra-helix in monomer subunit (b).

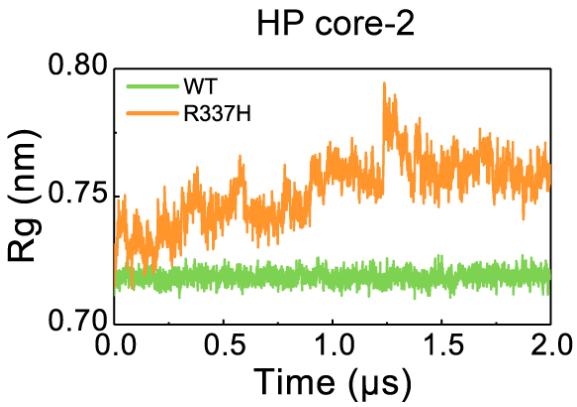

Fig. S9 The comparison of radius of gyration (Rg) of hydrophobic (HP) core-2 in dimer subunit as a function of time.

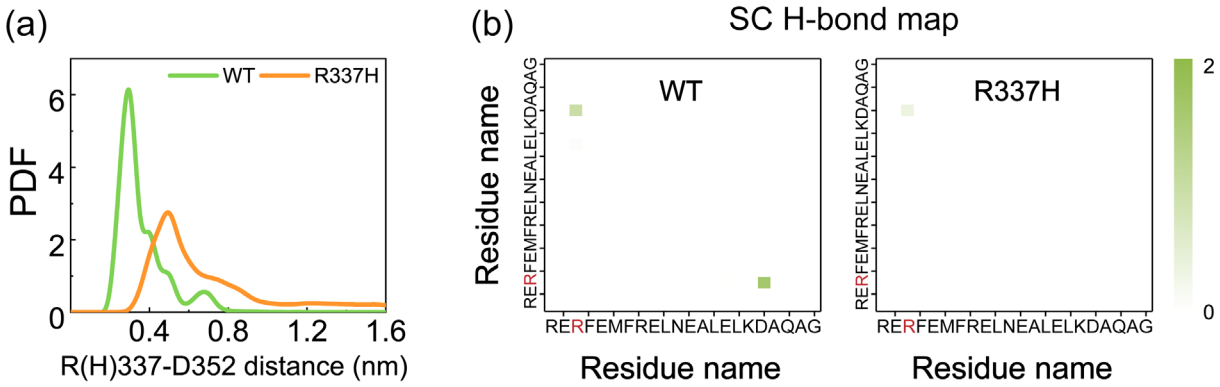

Fig. S10 (a) The PDF of distance between NH_2^+ group of R337 (or NH group of H337) and COO^- group of D352 (b) The SC H-bond number map of inter-helix in dimer subunit.

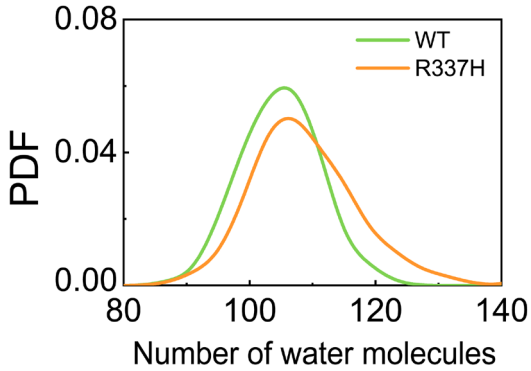

Fig. S11 The PDF of number of water molecules contacting with hydrophobic core of WT-p53Tet and its R337H mutant.

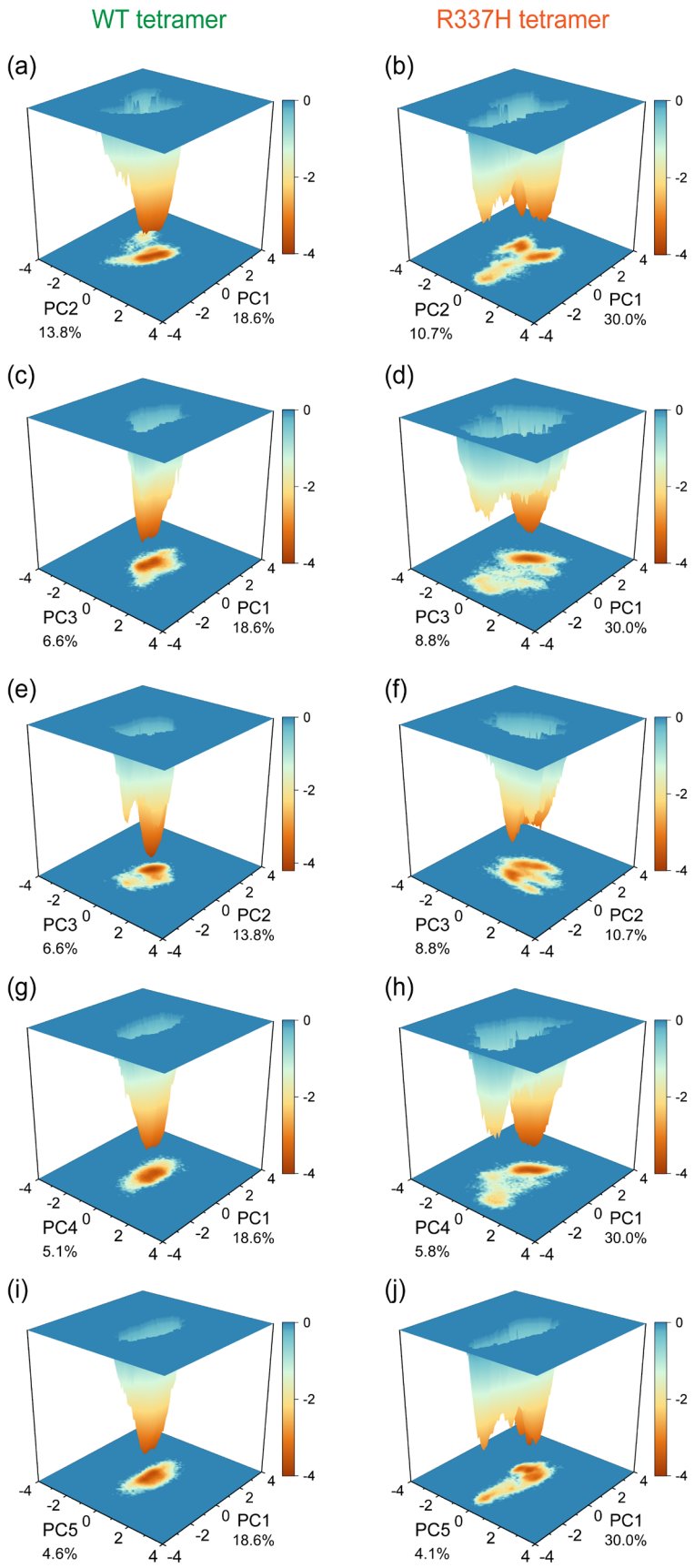

Fig. S12 The free energy landscape (in kcal/mol) projected onto the PC1-PC2 (a, b), PC1-PC3 (c, d), PC2-PC3 (e, f), PC1-PC4 (g, h) and PC1-PC5 (i, j) for WT-p53Tet and R337H-p53Tet.

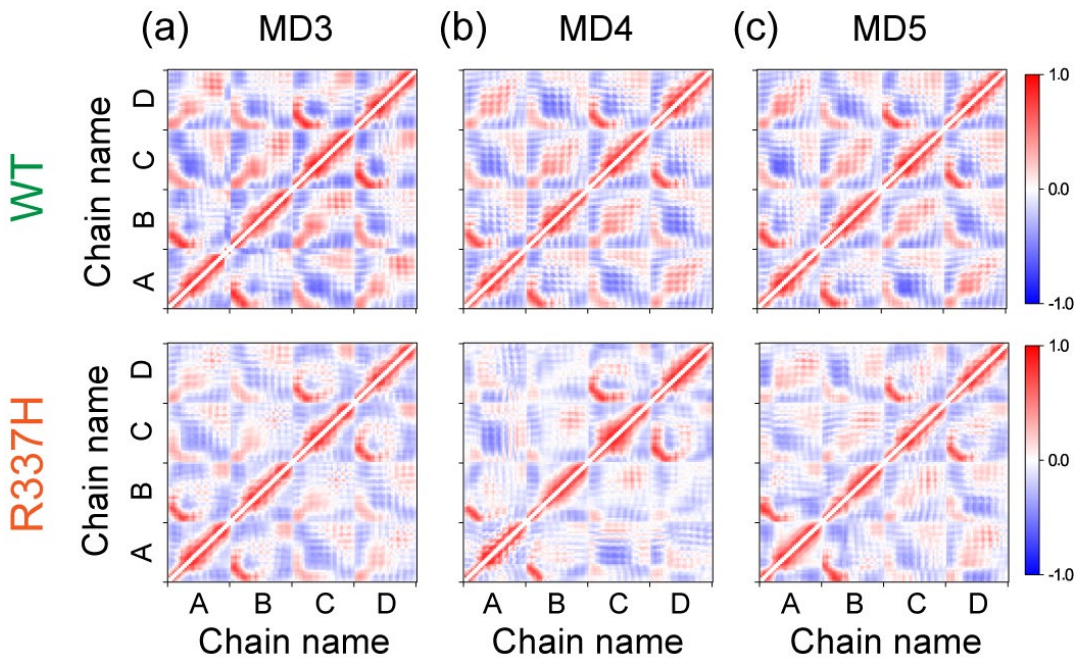

Fig. S13 (a-c) Residue-residue correlation maps from the other three MD runs of WT-p53Tet (upper) and R337H-p53Tet (lower).

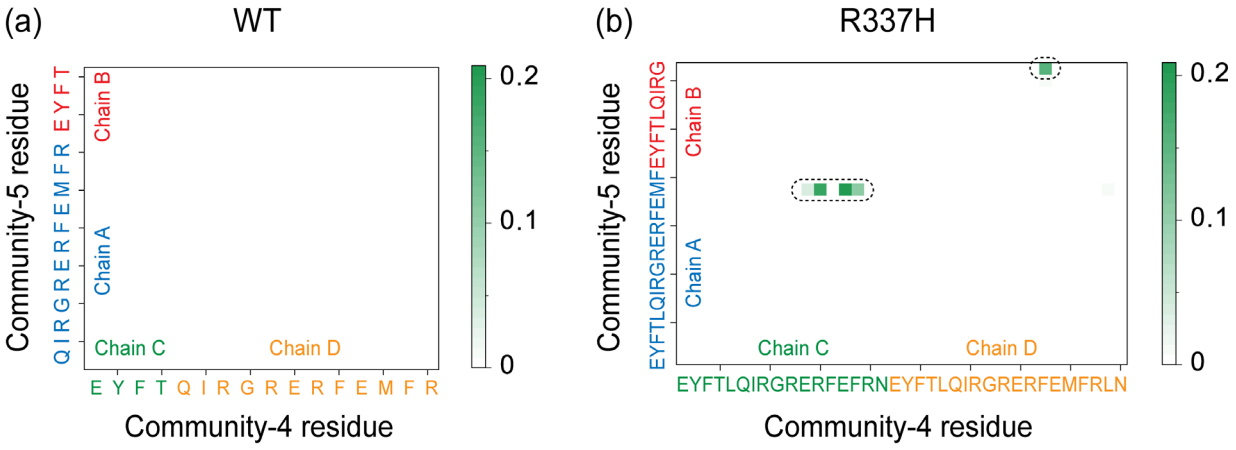

Fig. S14 The residue-based contact map between community-4 and community-5 for WT-p53Tet (a) and R337H-p53Tet (b).

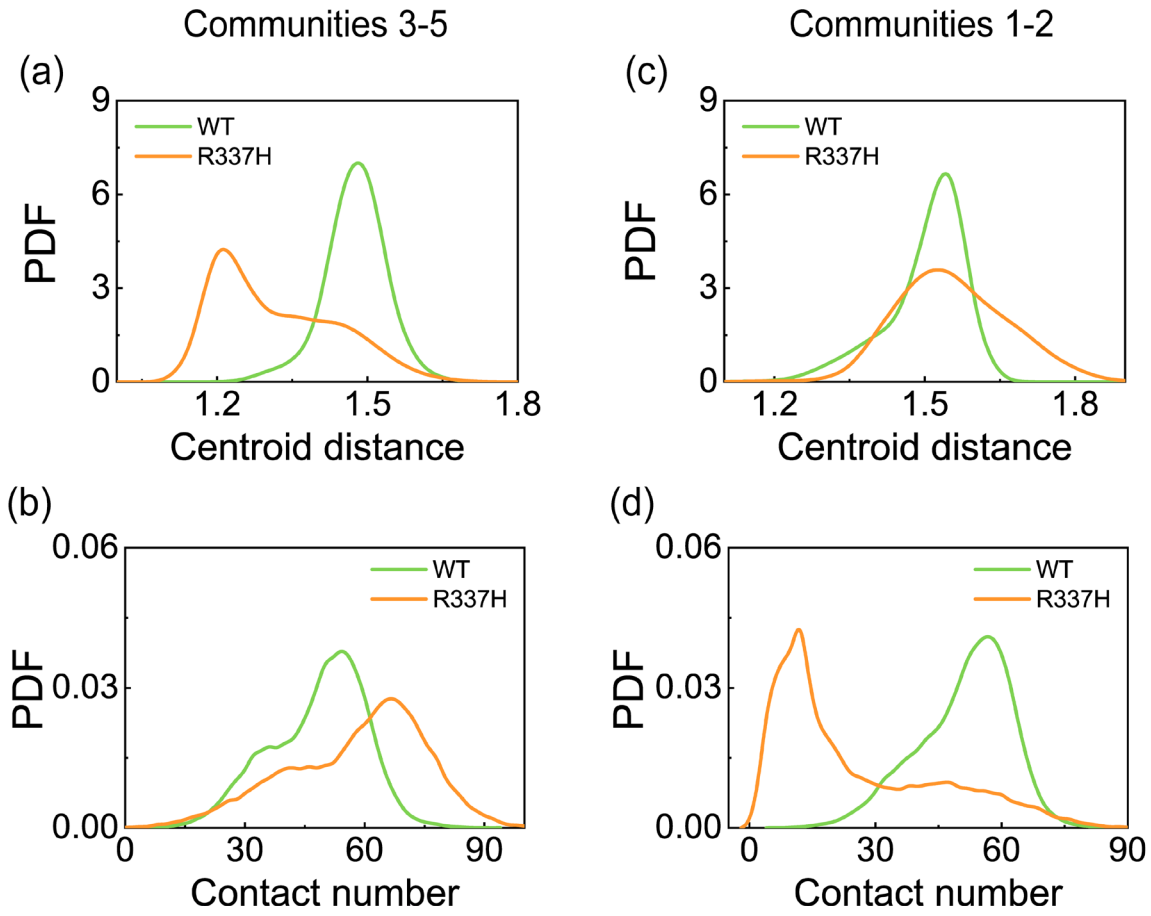

Fig. S15 The PDF of centroid distance (a, c) and of contact number (b, d) between the helix B (residues L344-G356) in community-3 and helix A (residues R335-R342) in community-5 (a, b) and between helix B (residues R335-N345) in community-1 and helix A (residues E343-G356) in community-2 (c, d).